NANOSYSTEMS: PHYSICS, CHEMISTRY, MATHEMATICS, 2020, 11 (3), P. 324–332

CeO_2 nanoparticles as free radical regulators in biological systems

M. M. Sozarukova[1], E. V. Proskurnina[2], A. E. Baranchikov[1], V. K. Ivanov[1]

[1]Kurnakov Institute of General and Inorganic Chemistry, Russian Academy of Sciences, Leninsky Prospect, 31, Moscow, 119991, Russia

[2]Research Centre for Medical Genetics, Moskvorechie St, 1, Moscow, 115522, Russia

s_madinam@bk.ru, proskurnina@gmail.com, a.baranchikov@yandex.ru, van@igic.ras.ru

PACS 68.65.k, 81.20.n, 82.70.Dd, 87.85.Rs **DOI 10.17586/2220-8054-2020-11-3-324-332**

Cerium dioxide nanoparticles possess unique physical and chemical properties, among which the enzyme-like activity is of particular interest. In particular, they are able to perform the functions of pro- and antioxidant enzymes, such as superoxide dismutase (SOD), catalase, and peroxidase. Due to the advantages associated with pH and temperature stability and low cost, CeO_2 nanoparticles can be considered as promising mimetics of these enzymes. In this paper, the antioxidant activity of a citrate-stabilized colloidal suspension of CeO_2 nanoparticles has been studied using chemiluminometry in model systems generating superoxide anion radical and hydrogen peroxide. In the lucigenin/xanthine/xanthine oxidase system, generating a superoxide anion radical, CeO_2 nanoparticles exhibit antioxidant properties increasing upon conjugation with SOD. When interacting with hydrogen peroxide, CeO_2 nanoparticles exhibit peroxidase-like activity. In the combined ROS generating system, lucigenin/Co(II)/H_2O_2, CeO_2 nanoparticles demonstrated prooxidant activity.

Keywords: cerium dioxide nanoparticles, superoxide anion radical, hydrogen peroxide, nanozymes, superoxide dismutase, peroxidase, chemiluminescence.

Received: 19 February 2020

1. Introduction

Enzymes are biocatalysts with high substrate specificity which increase the rate of biochemical reactions by several orders of magnitude. The catalytic properties of natural enzymes decrease in the presence of inhibitors, as well as with changes in temperature, pH, etc. One of the main limitations of the widespread use of enzymes is the high cost of their synthesis, isolation and purification [1]. Nanozymes have several advantages over natural enzymes, namely, high specificity and sensitivity, reproducibility of characteristics in a wide temperature and pH range, low cost, the possibility of additional functionalization and biocompatibility [2–5]. In this regard, at present, special attention of researchers is directed to the creation of enzyme mimetics based on nanoparticles – alternative systems that can effectively mimic the catalytic activity of natural enzymes.

The role of free radicals (reactive oxygen species, ROS) in the body is extremely high. They affect the physicochemical properties of biological membranes, their permeability and structure, are involved in cell signalling and maintenance of homeostasis, however, uncontrolled free radical processes can lead to cell damage [6]. Oxidative stress is defined as a pathological condition associated with excessive production of free radicals and their biochemically active intermediates and metabolites, exceeding the protective capabilities of the cell's antioxidant system and leading to destructive consequences for the cell and the organism as a whole [7]. The application of nanoparticles in experimental and clinical conditions is exponentially growing due to a wide range of their functional properties, but at the same time it increases the potentially unpredictable and adverse effects of their impact on the body [8]. Oxidative stress induced by nanoparticles leads to pathophysiological events such as damage to proteins, lipids, DNA, inflammation, cytotoxic effects, inhibition of antioxidant enzymes, activation of the radical-producing function of phagocytes, mitochondrial dysfunction and apoptosis [9].

Nanodisperse cerium dioxide is a promising material that is widely used in modern high-tech industries [10]. In recent years, some unique biochemical enzyme-like properties of cerium dioxide were revealed, which allow it to perform the functions of some natural enzymes such as superoxide dismutase, catalase, peroxidase. Numerous studies on cell cultures and animals have demonstrated the effective radical-scavenging properties of nanocrystalline CeO_2 [11–14]. The ability to act as a nanozyme in combination with relatively low toxicity makes CeO_2 nanoparticles a promising drug for the correction of oxidative stress. In this regard, it seems relevant and necessary to conduct comprehensive studies of CeO_2 nanoparticles as a catalyst/inhibitor of free radical reactions.

One of the most important primary free radicals is the superoxide anion radical. The dismutation of superoxide anion radicals inevitably leads to the formation of hydrogen peroxide molecules that can easily penetrate cell membranes. Recently, more and more attention has been paid to the role of hydrogen peroxide, not only as a cytotoxic component found during phagocytosis, the activity of mitochondria and microsomes, but also to its participation in

the regulation of cellular signalling and transcription factors. Thus, in the present work, we have comprehensively studied the enzyme-like properties of the citrate-stabilized CeO_2 sol with respect to two key participants in the free radical homeostasis – superoxide anion radical and hydrogen peroxide, using the sensitive, informative, and express chemiluminescent method. Moreover, the study involved both standalone biochemical models for generation of $\cdot O_2^-$ and H_2O_2, and a combined ROS-generating system containing their mixture.

2. Materials and methods

2.1. Synthesis and physicochemical study of citrate-stabilized CeO_2 sol

The synthesis of citrate stabilized cerium dioxide sol was carried out according to the procedure based on the thermohydrolysis of the aqueous solution of ammonium cerium(IV) nitrate [15]. Aqueous solution of $(NH_4)_2Ce(NO_3)_6$ (extra pure grade, Sigma-Aldrich, USA) with a concentration of 100 g/l was kept for 24 h in an oven at 95 °C. The formed precipitate was separated from the mother liquor by centrifugation followed by triple washing with isopropanol. The washed precipitate was redispersed in deionized water, followed by boiling for 1 h with constant stirring until complete removal of isopropanol. The concentration of the CeO_2 sol was determined by the thermogravimetric method. The obtained colloidal solution of CeO_2 was stabilized with ammonium citrate $C_6H_{14}O_7N_2$ (disubstituted ammonium citrate, extra-pure grade, Sigma-Aldrich, USA) with 1:1 molar ratio.

The citrate-stabilized cerium dioxide sol was analyzed by X-ray diffraction (XRD), transmission electron microscopy (TEM) and dynamic light scattering (DLS). X-ray diffraction analysis of nanocrystalline CeO_2 samples was carried out on a Bruker D8 Advance diffractometer (CuKα radiation, θ–2θ geometry). The diffraction peaks were identified using the ICDD PDF2 data bank. The average hydrodynamic diameter of CeO_2 nanoparticles was estimated by the DLS method using a Photocor Complex analyzer. The microstructure of the samples was studied by TEM on a Leo 912 AB Omega electron microscope at an accelerating voltage of 100 kV.

2.2. Synthesis of superoxide dismutase conjugated with cerium dioxide nanoparticles

A stock solution of superoxide dismutase (SOD, Sigma-Aldrich, USA, S8160-15KU) with an activity of 2400 U/ml ($c = 25$ μM) was obtained by dissolving a portion of SOD in deionized water. The SOD–CeO_2 conjugate was prepared according to the procedure described by Gil et al. [16]. A SOD working solution with an activity of 100 U/ml ($c = 1$ μM) was mixed with 12 mM citrate-stabilized CeO_2 sol. The resulting mixture was incubated at room temperature in a dark place for 1 and 2.5 hours. To determine the possible effect of citrate ions, a SOD-ammonium citrate mixture with corresponding concentration was prepared the similar way. Individual solutions of SOD, ammonium citrate, and stabilized CeO_2 sol were incubated together with conjugates, under the same conditions.

2.3. Study of SOD-like activity by the chemiluminescent method in the lucigenin/xanthine/xanthine oxidase system

2.3.1. Preparation of solutions. SOD-like activity was determined by chemiluminometry in the xanthine/xanthine oxidase model system in the presence of a chemiluminescent probe, lucigenin, which is selective for the superoxide anion radical. Phosphate buffer solutions (PBS) with a concentration of 100 mM and a pH of 7.4 and 8.6 were prepared by dissolving a weighed portion of KH_2PO_4 (Sigma-Aldrich, USA) in 1.00 L of distilled water, followed by adjusting to the desired pH using granular KOH (Sigma-Aldrich, USA) and/or concentrated HCl solution (Sigma-Aldrich, USA).

Solutions of xanthine (3,7-dihydropurin-2,6-dione, Sigma-Aldrich, USA) and lucigenin (10,10'-dimethyl-9.9'-bicridinium dinitrate, Sigma-Aldrich, USA) with working concentrations of 1 mM were prepared by dissolving weighed portions in the PBS with a pH 8.6 and 7.4, respectively. A xanthine oxidase working solution (Sigma-Aldrich, USA, X1875-25UN) with an activity of 0.11 U/ml was prepared by diluting the initial PBS suspension (pH 7.4). Before CL-measurements, the working solution of the enzyme was kept for 15 min at room temperature. By definition of catalytic activity, one unit of the enzyme in 1 min converts 1.0 μmol of xanthine to uric acid at 25 °C and a pH of 7.5.

2.3.2. Registration of chemiluminescence. Chemiluminescence was recorded on a Lum-100 single-channel chemiluminometer (DISoft, Russia) at 37 °C. Aliquots of xanthine ($c = 25$ μM), lucigenin ($c = 25$ μM) and the analyzed sample were added to a plastic cuvette containing PBS ($c = 100$ mM, pH 7.4). The background glow was recorded for 30 – 60 s, then an aliquot of xanthine oxidase ($a = 11$ mU/ml) was added. The total volume of the system was 1000 ml. Each experimental point presented in the work was obtained in no less than three parallel experiments ($n = 3$). The original PowerGraph software product was used to conjugate the computer and the instrument.

The light sum was used as an analytical signal – the area under the CL curve for a certain period of time (5 min).

2.4. The study of peroxidase/catalase activity by the chemiluminescent method in the luminol/H_2O_2 system

2.4.1. Preparation of solutions. The peroxidase/catalase activity of the analysed samples was studied in the luminol/H_2O_2 system. A solution of luminol (5-amino-1,2,3,4-tetrahydro-1,4-phthalazinedione, 3-aminophthalic acid hydrazide, Sigma-Aldrich, USA) with $c = 1$ mM was prepared by dissolving a sample in PBS (pH 7.4). A working solution of hydrogen peroxide with a concentration of 2.5 M was prepared by diluting 33 % H_2O_2 stock solution (Sigma-Aldrich, USA) with distilled water.

2.4.2. Registration of chemiluminescence. Chemiluminescence was recorded on a single-channel Lum-100 chemiluminometer at room temperature. Aliquots of luminol ($c = 50$ μM) and the analysed sample were added to a plastic cuvette containing PBS ($c = 100$ mM, pH 7.4). The background glow was recorded for 30 – 60 s, then an aliquot of H_2O_2 was added ($c = 50$ mM). The total volume of the system was 1000 ml. Each experimental point presented in the work was obtained in no less than three parallel experiments ($n = 3$).

2.5. The study of pro- and antioxidant activity in the lucigenin/Co(II)/H_2O_2 system

2.5.1. Preparation of solutions. An analytical model of lucigenin/Co(II)/H_2O_2 was used as a combined ROS generation system (includes a superoxide anion radical, hydrogen peroxide, hydroxyl radical).

Co(II) solutions with a concentration of 20 mM were prepared by dissolving a weighed portion of $CoCl_2 \cdot 6H_2O$ (Sigma-Aldrich, USA) in distilled water. A solution of dithiothreitol ((2*S*, 3*S*)-1,4-bis(sulfanyl)butane-2,3-diol, Sigma-Aldrich, USA) with a concentration of 30 mM was obtained by dissolving a sample in distilled water. A working solution of hydrogen peroxide with a concentration of 0.3 M was prepared by diluting 33 % H_2O_2 stock solution with distilled water.

2.5.2. Registration of chemiluminescence. Chemiluminescence was recorded on a 12-channel Lum-1200 chemiluminometer (DISoft, Russia) at room temperature. Aliquots of Co(II) ($c = 0.6$ mM), lucigenin ($c = 0.1$ mM) and the analysed sample were added to a cuvette containing PBS ($c = 100$ mM, pH 8.6). The background glow was recorded for 30 – 60 s, then, without interrupting the recording of the analytical signal, an aliquot of H_2O_2 ($c = 3.0$ mM) was introduced into the system. The total volume of the system was 1000 ml. Each experimental point presented in the work was obtained in no less than three parallel experiments ($n = 3$).

The light sum in 20 min was used as an analytical signal.

3. Results and discussion

An electrostatically stabilized sol of nanocrystalline cerium dioxide was obtained by thermohydrolysis of an aqueous solution of ceric ammonium nitrate. The CeO_2 content in the sol was 23 g/L (0.13 M). According to XRD data, the obtained sol contained single phase cerium dioxide (PDF2 34-0394). The particle size, estimated by the Scherrer ratio, was 3 nm. The average hydrodynamic diameter of the nanoparticles obtained by the DLS method was found to be 10 – 11 nm. Data on the particle size and phase composition of the obtained material were confirmed by the results of TEM and electron diffraction analysis of the CeO_2 sol.

The antioxidant activity of the samples of citrate-stabilized CeO_2 sol, SOD, CeO_2–SOD and ammonium citrate-SOD conjugates at the time of preparation and after incubation for 1 and 2.5 hours at room temperature was evaluated using the chemiluminescent method in the xanthine/xanthine oxidase system in the presence of lucigenin and a selective CL probe for a superoxide anion radical. Fig. 1 shows chemiluminograms for various concentrations of CeO_2 nanoparticles. The addition of a citrate-stabilized cerium dioxide sol to the lucigenin/xanthine/xanthine oxidase system led to a decrease in the stationary level of CL, which indicates the presence of SOD-like activity. Earlier, we estimated the SOD-like activity of 1 mmol/L citrate-stabilized colloidal solution of CeO_2 in units of SOD activity, amounting 2.00 ± 0.03 nmol/L, which is approximately 6 orders of magnitude lower than the activity of the native enzyme.

Similar chemiluminograms are recorded when SOD is introduced into the system (Fig. 2a). The effect of luminescence quenching linearly depends on the concentration of SOD (Fig. 2b):

$$\Delta S,\ (\times 10^3 \text{ imp}) = S_0 - S = (3.9 \pm 0.6) \times c\ (\text{SOD},\ \text{nmol/l}) + (6.8 \pm 1.0),\ r = 0.992\ (P = 0.95,\ n = 5),$$

where S_0 and S are light sums for the control and experiment, respectively.

Based on the study of the antioxidant properties of individual samples of citrate-stabilized CeO_2 sol and individual SOD, working concentrations were selected (c (CeO_2, ammonium citrate) = 0.12 mM, and (SOD) = 1 U/ml, a (SOD) = 10 nM) and CeO_2-SOD, ammonium citrate-SOD conjugates were prepared. Relative ΔS_{rel} value was calculated from chemiluminograms (Fig. 3), according to the formula:

$$\Delta S_{rel},\ \% = \frac{S_0 - S}{S_0} \times 100\ \%,$$

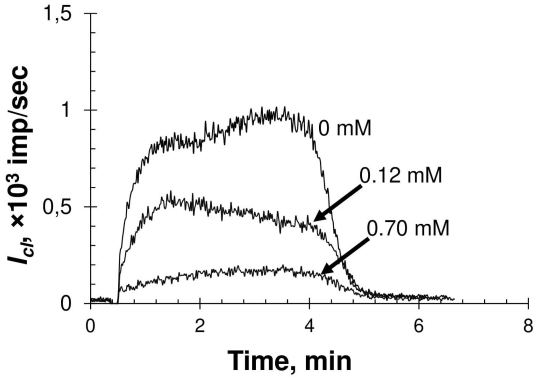

FIG. 1. Chemiluminograms of a citrate-stabilized colloidal solution of CeO_2 (concentrations are shown in the figure) in the lucigenin (25 μM) + xanthine (25 μM) + xanthine oxidase (11 mU/ml) system

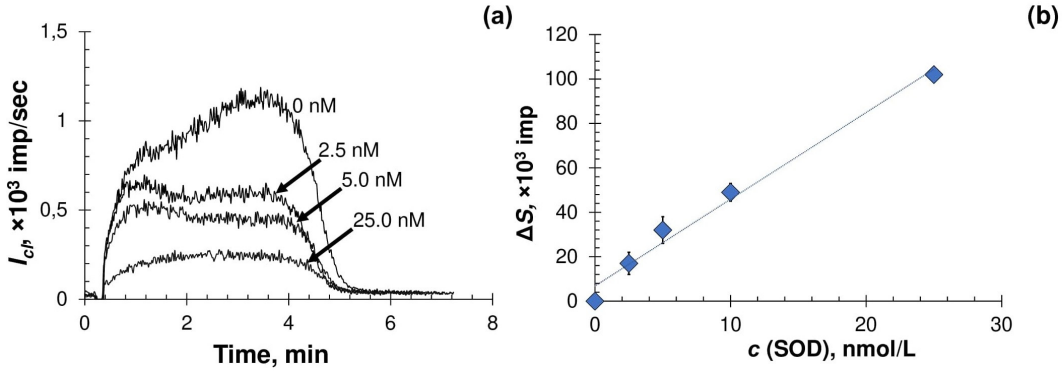

FIG. 2. (a) CL-curves for SOD (concentrations are shown in the figure) in the system containing lucigenin (25 μM) + xanthine (25 μM) + xanthine oxidase (11 mU/ml), (b) the area difference (ΔS) under the CL curves, proportional to the number of captured superoxide anion radicals, as a function of the SOD concentration; light sum was calculated in 5 min

where S_0 and S are light sums for the control and experiment, respectively.

According to the data obtained, the CeO_2-SOD conjugate exhibits increased enzyme-like activity which does not depend on the incubation time, more effectively inhibiting superoxide anion radicals in comparison with the citrate-stabilized colloidal CeO_2 solution and individual superoxide dismutase. This result indicates the synergistic effect of CeO_2 nanoparticles and SOD absorbed on their surface, which is in good agreement with published data [16, 17].

Superoxide anion radical (SAR) is one of the primary free radicals formed in living systems. The main sources of SAR in the cell are mitochondria and enzyme systems: xanthine oxidase [18], lipoxygenase [19], cyclooxygenase [20, 21], NADPH oxidase [22]. The SAR serves as a precursor to other active forms of oxygen – hydrogen peroxide, hydroxyl radical, peroxynitrite [23]. For normal functioning a certain level of SAR must be maintained in the cell, however, its uncontrolled formation during pathology can lead to the development of lipid oxidative stress, damage to membranes and cellular apoptosis.

Superoxide dismutase catalyses the disproportionation of superoxide radical anions to molecular oxygen and hydrogen peroxide. The mechanism of SOD action is presented by the following partial reactions (1), (2):

$$\mathrm{M^{(n+1)} - SOD + {\cdot}O_2^- \rightarrow Mn^+ - SOD + O_2}, \tag{1}$$

$$\mathrm{M^{n+} - SOD + {\cdot}O_2^- + 2H^+ \rightarrow M^{(n+1)} - SOD + H_2O_2}, \tag{2}$$

where M is a transition metal cofactor of the active center of the enzyme (Cu, Mn, Fe, and Ni) [1, 24]. The most common type of enzyme in eukaryotic cells is Cu,Zn-SOD, localized in the cytosol [1, 25].

The ability to catalyze the dismutation of superoxide anion radical was one of the first discovered enzyme-like properties of nanocrystalline cerium dioxide [26–29]. The obtained results indicate the important role of the surface state (the presence of Ce(III) in the surface layer) and the size (smaller particles showed greater activity) of CeO_2 nanoparticles. Several methods have been proposed for increasing the SOD-like activity of nanocrystalline CeO_2. Lee

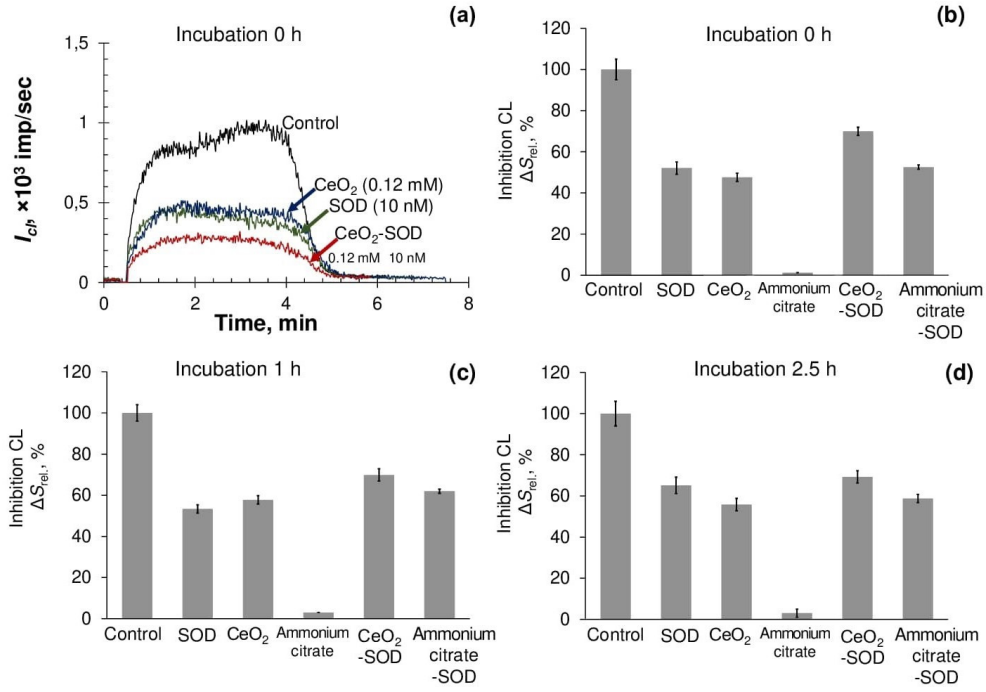

FIG. 3. (a) Chemiluminograms of a citrate-stabilized CeO_2 sol, native SOD, and CeO_2-SOD conjugate (concentrations are shown in the figure, incubation for 0 h) in the lucigenin system (25 μM) + xanthine (25 μM) + xanthine oxidase (11 mU/ml), (b), (c), (d) – the degrees of free radical inhibition by native SOD (10 nM), citrate-stabilized CeO_2 sol (0.12 mM), ammonium citrate (0.12 mM), CeO_2-SOD and ammonium citrate-SOD conjugates calculated on the basis of the recorded CL curves when incubated for 0, 1, and 2.5 hours, respectively. The light sum was calculated in 5 min

et al. [17] showed that the SOD-like activity of cerium dioxide nanoparticles significantly increased after incubation with Cu,Zn-SOD or with an electron-donating molecule $[Ru(dcbpy)_2(NCS)_2]$. The EPR data showed a 6–12-fold enhanced SOD-mimetic activity upon conjugation of 33 nm nanoparticles of CeO_2 with 20 U/ml Cu,Zn-SOD in PBS [17]. Singh et al. [30] found that the enzyme-like activity of CeO_2 nanoparticles does not change after their modification with bovine serum albumin and polyethylene glycol. In addition, Singh et al. have encapsulated CeO_2 nanoparticles in a polyethylene glycol matrix, after release from which the nanoparticles also retained SOD mimetic activity. These and other studies indicate that organic ligands or biomolecules used to stabilize CeO_2 nanoparticles do not interfere with the manifestation of the antioxidant properties of the latter.

The second key participant in free radical reactions in living systems is hydrogen peroxide. To evaluate the catalase-/peroxidase-like activity of a citrate-stabilized colloidal solution of CeO_2, the lucigenin/H_2O_2 and luminol/H_2O_2 systems were studied (Fig. 4). The lucigenin/H_2O_2 system is characterized by stationary kinetics of luminescence, which does not change when CeO_2 sol is introduced into the system. Thus, under the chosen conditions, the CeO_2 sol does not exhibit catalase properties. In the luminol/H_2O_2 system, a dose-dependent increase in the luminescence intensity was observed with an increase in the concentration of the added citrate-stabilized CeO_2 sol, which indicates the manifestation of peroxidase activity by cerium dioxide.

According to existing data, at pH > 6.0 CeO_2 nanoparticles do not demonstrate peroxidase-like properties [31]. However, for stoichiometric cerium dioxide nanoparticles obtained by high-temperature treatment, this type of nanozyme activity was still observed at higher pH values. It was shown that due to peroxidase-like activity, CeO_2 nanoparticles (20 – 30 nm) at pH 7.2 accelerated the interaction of H_2O_2 with luminol, enhancing its luminescence [32]. In this case, cerium perhydroxide, decomposing with the formation of superoxide and hydroxyl radicals in the absence of Ce^{3+} ions, is presumably formed as an intermediate on the surface of the particles.

Peroxidases are glycoproteins that catalyse the oxidation of various organic and inorganic substrates using hydrogen peroxide as an electron acceptor. In biological systems, there are many types of peroxidases, such as glutathione peroxidase, lactoperoxidase, peroxyredoxins, myeloperoxidase, haloperoxidase, etc. [1]. The peroxidase-like activity of nanomaterials is used to detect hydrogen peroxide [5], glucose [33, 34], lead ions [35] and mercury ions [36], DNA methylation [37], as well as for immunoassay applications [38]. The classic work on the peroxidase-like activity of

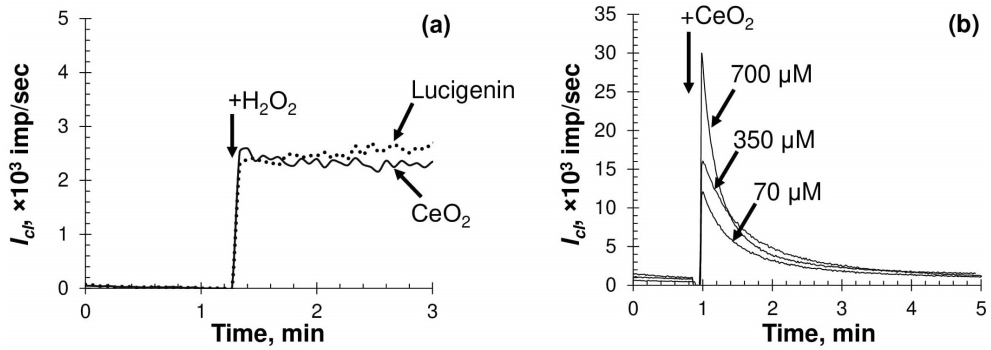

FIG. 4. Chemiluminograms of systems containing (a) lucigenin (0.1 mM) and a citrate-stabilized CeO_2 sol (700 μM) after the addition of H_2O_2 (3.0 mM), (b) luminol (50 μM) + H_2O_2 (50 mM) and a citrate-stabilized CeO_2 sol (concentrations are shown in the figure) after the addition of H_2O_2 (3.0 mM)

CeO_2 is an article by Jiao et al. [31], in which, based on the studied peroxidase activity of the CeO_2 sol, the prospect was substantiated of its application in the glucose test for oxidizing the substrate instead of horseradish peroxidase. Another successful practical application of this type of nanozyme activity is the combined use of CeO_2 nanoparticles and horseradish peroxidase for production of H_2O_2 sensors [9]. In a recent study, Vinothkumar et al. [5] demonstrated the possibility of using $CePO_4$–CeO_2 composite nanorods, which are peroxidase mimetics, for the detection of glucose and H_2O_2 by the colorimetric method with a high sensitivity.

At the final stage of our investigation, we studied the enzyme-like activity of cerium dioxide in the combined model — Co(II)/H_2O_2 in the presence of lucigenin. The system simultaneously contained hydrogen peroxide, superoxide anion radical and hydroxyl radical [40]:

$$\mathrm{Co^{2+} + H_2O_2 \rightarrow Co^{3+} + OH^- + \cdot OH}, \tag{3}$$

$$\mathrm{Co^{3+} + H_2O_2 \rightarrow Co^{2+} + 2H^+ + \cdot O^{2-}}. \tag{4}$$

Hydroxyl radicals have the highest oxidative activity among all other ROS. They can cause DNA damage, oxidative carbonylation of proteins and peroxidation of lipids, which, ultimately, can lead to inflammatory and oncological diseases, as well as aging [41]. In biological systems, there are no specific enzymes to scavenge hydroxyl radicals; yet some researchers suggest that this function is performed by such antioxidants as SOD, catalase, glutathione peroxidase, melatonin, and vitamin E [1]. More recently, there have been reports of the radical-intercepting properties of CeO_2 nanoparticles with respect to hydroxyl radicals [42, 43].

When H_2O_2 was added to the PBS medium (pH 8.6) containing Co(II) and lucigenin, the CL growth kinetics was observed, the intensity of which was proportional to the concentrations of $CoCl_2$ and H_2O_2 (Fig. 5).

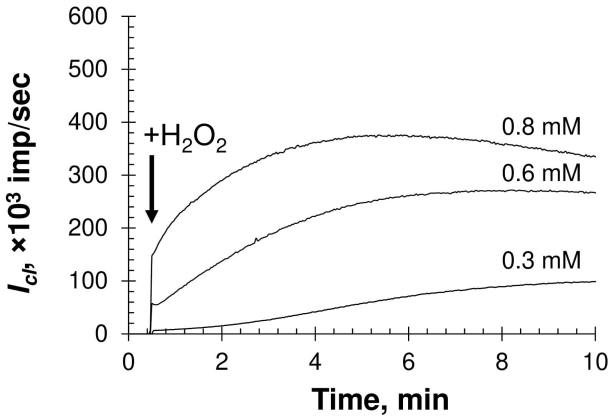

FIG. 5. Chemiluminograms for a system containing lucigenin (0.1 mM), Co(II) (concentrations are shown in the figure) and H_2O_2 (3.0 mM)

In the presence of SOD, luminescence quenching was observed due to the capture of the superoxide anion radical (Fig. 6a). A sulfhydryl compound, dithiothreitol, which also exhibited an inhibitory effect, was used as a selective inhibitor of the hydroxyl radical (Fig. 6b).

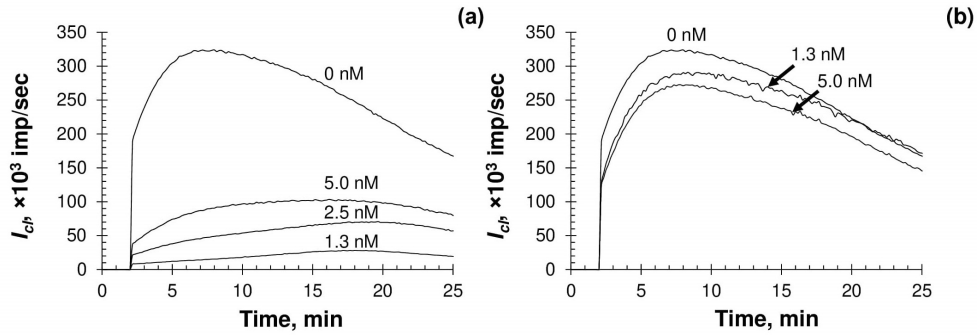

FIG. 6. Chemiluminograms for the system containing lucigenin (0.1 mM) + Co(II) (0.6 mM) + H_2O_2 (3.0 mM) in the presence of (a) SOD and (b) dithiothreitol (concentrations are shown in the figure)

The chemiluminograms obtained by adding a citrate-stabilized CeO_2 sol to the system, as well as the dependence of the light sum on the concentration of the analysed sample in the linear region, are shown in Fig. 7(a, b).

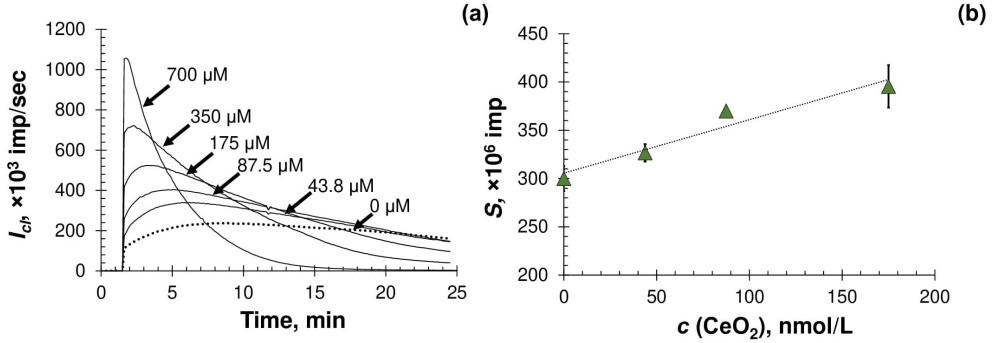

FIG. 7. (a) Chemiluminograms of a citrate-stabilized colloidal solution of CeO_2 (concentrations are shown in the figure) in the system containing lucigenin (0.1 mM) + Co(II) (0.6 mM) + H_2O_2 (3.0 mM), (b) the light sum (S) dependence under the CL curves on the concentration of CeO_2 nanoparticles. The light sum was calculated in 20 min

According to the data obtained, CeO_2 nanoparticles in the lucigenin/Co(II)/H_2O_2 system exhibit prooxidant properties, apparently due to peroxidase activity. With an increase in the concentration of CeO_2 sol introduced into the system, an increase in CL intensity was observed, and saturation occurred at a certain moment.

Thus, in relation to the two main active forms of oxygen – superoxide anion radical and hydrogen peroxide – cerium dioxide exhibits multidirectional activity. Judging by the published data, the pro- and antioxidant properties of CeO_2 nanoparticles are closely related. The determining factors are stoichiometry, redox potential of CeO_2 nanoparticles, pH of the medium, the presence of H_2O_2, etc. [44]. In a recent paper [45], calculations of the difference in redox potentials made it possible to evaluate the protective effect of CeO_2 nanoparticles against H_2O_2, taking into account the pH in the cell and organelles. It is possible to control the pro- and antioxidant properties of cerium dioxide nanoparticles in a wide range of pH values typical to biological media by changing the stoichiometry, design and strategy of synthesis [44, 46, 47]. The maximum prooxidant effect of CeO_2 was observed for the contents of vesicles – lysosomes and endosomes (pH < 6.2) [45]. Prooxidant properties may be useful for the destruction of undesirable exogenous components (toxins, bacteria, viruses), since it is the vesicular absorption mechanism that provides the bulk of the substances into the eukaryotic cell [44]. Analysis of the pH-dependent redox behavior of CeO_2 nanoparticles allows us to conclude that they provide the maximum protective potential against oxidative stress in mitochondria. Currently, evidence has been obtained of the effectiveness of targeted antioxidant therapy of mitochondrial dysfunctions to protect cells under conditions of oxidative stress and aging [48].

4. Conclusion

Oxidative stress underlies many neurodegenerative, cardiovascular, immune diseases, hormonal disorders, and a number of pathological conditions, including inflammation, hypoxia, tumor growth and aging. Numerous studies show that in fact there is not a single disease in which an imbalance of redox homeostasis would not be manifested, in some cases being the cause or primary part of pathogenesis, in others being the consequence. The development of new drugs – regulators of free-radical balance, among which nanodrugs play an important role, is gaining increasing popularity. The prospect of biomedical use of the nanodrugs is due to many unique advantages associated with pharmacokinetics, biodistribution, stable antioxidant activity, etc. [49]. To achieve maximum diagnostic and therapeutic efficacy, the activity of nanozymes can be remotely controlled using external stimuli, including exposure to magnetic field, light, ultrasound, and heat [50].

The increased interest in CeO_2 nanoparticles is due to the unique combination of physicochemical and nanozyme properties that these particles possess. Promising preclinical therapeutic effects require a comprehensive safety analysis of CeO_2 nanoparticles – toxicity and effects on free radical homeostasis. As follows from the study, the pro- and antioxidant properties of cerium dioxide nanoparticles are closely related. The results obtained after assessing relative safety indicate the prospects for the use of CeO_2 nanoparticles as free radical regulators, for example, in redox therapy of cancer.

Acknowledgements

This work was supported by the Russian Science Foundation (project No. 19-13-00416).

References

[1] Yadav N., Patel V., Singh S. Cerium Oxide-Based Nanozymes in Biology and Medicine. *Springer Proceedings in Physics*, 2018, **236**, P. 193–213.
[2] Gao L., Zhuang J., et al. Intrinsic peroxidase-like activity of ferromagnetic nanoparticles. *Nat. Nanotechnol.*, 2007, **2** (9), P. 577–583.
[3] Chen T.M., Tian X.M., et al. Nanodiamonds as pH-switchable oxidation and reduction catalysts with enzyme-like activities for immunoassay and antioxidant applications. *Nanoscale*, 2017, **9** (40), P. 15673–15684.
[4] Cho S., Shin H.Y., Kim M.I. Nanohybrids consisting of magnetic nanoparticles and gold nanoclusters as effective peroxidase mimics and their application for colorimetric detection of glucose. *Biointerphases*, 2017, **12** (1), P. 01A401–01A407.
[5] Vinothkumar G., Lalitha A.I., Suresh Babu K. Cerium Phosphate-Cerium Oxide Heterogeneous Composite Nanozymes with Enhanced Peroxidase-Like Biomimetic Activity for Glucose and Hydrogen Peroxide Sensing. *Inorg. Chem.*, 2019, **58** (1), P. 349–358.
[6] Naito Y., Yoshikawa T. Molecular and cellular mechanisms involved in Helicobacter pylori-induced inflammation and oxidative stress. *Free Radic. Biol. Med.*, 2002, **33** (3), P. 323–336.
[7] Sies H., Cadenas E. Oxidative stress: damage to intact cells and organs. *Philos. Trans. R. Soc. Lond. B Biol. Sci.*, 1985, **311** (1152), P. 617–631.
[8] Yildirimer L., Thanh N.T., et al. Toxicology and clinical potential of nanoparticles. *Nano Today*, 2011, **6** (6), P. 585–607.
[9] Ganguly R., Singh A.K., et al. *Nanotechnology in Modern Animal Biotechnology*. Elsevier, 2019, 178 p.
[10] Ivanov V.K., Polezhaeva O.S., Tret'yakov Yu.D. Nanocrystalline ceria: Synthesis, structure-sensitive properties, and promising applications. *Russ. J. Gen. Chem.*, 2010, **80**, P. 604–617.
[11] Grulke E., Reed K., et al. Nanoceria: factors affecting its pro- and anti-oxidant properties. *Environ. Sci. Nano*, 2014, **1**, P. 429–444.
[12] Popov A.L., Popova N.R., et al. Cerium oxide nanoparticles stimulate proliferation of primary mouse embryonic fibroblasts in vitro. *Mater. Sci. Eng. C*, 2016, **68**, P. 406–413.
[13] Zholobak N.M., Shcherbakov A.B., et al. Panthenol-stabilized cerium dioxide nanoparticles for cosmeceutic formulations against ROS-induced and UV-induced damage. *J. Photochem. Photobiol. B*, 2014, **130**, P. 102–108.
[14] Shcherbakov A.B., Zholobak N.M., Spivak N.Ya., Ivanov V.K. Advances and prospects of using nanocrystalline ceria in cancer theranostics. *Russ. J. Inorg. Chem.*, 2014, **59**, P. 1556–1575.
[15] Shcherbakov A.B., Teplonogova M.A., et al. Facile method for fabrication of surfactant-free concentrated CeO_2 sols. *Mater. Res. Express*, 2007, **4** (5), P. 4–14.
[16] Gil D., Rodriguez J., et al. Antioxidant Activity of SOD and Catalase Conjugated with Nanocrystalline Ceria. *Bioengineering*, 2017, **4** (18), P. 1–9.
[17] Li Y., He X., et al. Acquired superoxide-scavenging ability of ceria nanoparticles. *Angew. Chem. Int. Ed. Engl.*, 2015, **54** (6), P. 1832–1835.
[18] Kuppusamy P., Zweier J.L. Characterization of free radical generation by xanthine oxidase. Evidence for hydroxyl radical generation. *J. Biol. Chem.*, 1989, **264** (17), P. 9880–9884.
[19] Phaniendra A., Jestadi D.B., Periyasamy L. Free radicals: properties, sources, targets, and their implication in various diseases. *Indian J. Clin. Biochem.*, 2015, **30** (1), P. 11–26.
[20] Kontos H.A., Wei E.P. et al. Appearance of superoxide anion radical in cerebral extracellular space during increased prostaglandin synthesis in cats. *Circ. Res.*, 1985, **57** (1), P. 142–151.
[21] McIntyre M., Bohr D.F., Dominiczak A.F. Endothelial function in hypertension: the role of superoxide anion. *Hypertension*, 1999, **34** (4 Pt 1), P. 539–545.
[22] Babior B.M., Lambeth J.D., Nauseef W. The neutrophil NADPH oxidase. *Arch. Biochem. Biophys.*, 2002, **397** (2), P. 342–344.
[23] Kawano T., Kagenishi T., et al. Production and removal of superoxide anion radical by artificial metalloenzymes and redox-active metals. *Commun. Integr. Biol.*, 2015, **8** (6), P. e1000710.
[24] Lu J.M., Lin P.H., et al. Chemical and molecular mechanisms of antioxidants: experimental approaches and model systems. *J. Cell. Mol. Med.*, 2010, **14** (4), P. 840–860.

[25] Perry J.J., Shin D.S., et al. The structural biochemistry of the superoxide dismutases. *Biochim. Biophys. Acta*, 2010, **1804** (2), P. 245–262.
[26] Tarnuzzer R.W., Colon J., et al. Vacancy engineered ceria nanostructures for protection from radiation-induced cellular damage. *Nano Lett.*, 2005, **5** (12), P. 2573–2577.
[27] Korsvik C., Patil S., et al. Superoxide dismutase mimetic properties exhibited by vacancy engineered ceria nanoparticles. *Chem. Commun. (Camb.)*, 2007, **10**, P. 1056–1058.
[28] Heckert E.G., Karakoti A.S., et al. The role of cerium redox state in the SOD mimetic activity of nanoceria. *Biomaterials*, 2008, **29** (18), P. 2705–2709.
[29] Karakoti A.S., Singh S., et al. PEGylated nanoceria as radical scavenger with tunable redox chemistry. *J. Am. Chem. Soc.*, 2009, **131** (40), P. 14144–14145.
[30] Singh V., Singh S., et al. A facile synthesis of PLGA encapsulated cerium oxide nanoparticles: release kinetics and biological activity. *Nanoscale*, 2012, **4** (8), P. 2597–2605.
[31] Jiao X., Song H., et al. Well-redispersed ceria nanoparticles: Promising peroxidase mimetics for H_2O_2 and glucose detection. *Analytical Methods*, 2012, **4**, P. 3261–3267.
[32] Xiaohua L., Zhang Zh., et al. A Chemiluminescence Microarray Based on Catalysis by CeO_2 Nanoparticles and Its Application to Determine the Rate of Removal of Hydrogen Peroxide by Human Erythrocytes. *Appl. Biochem. Biotechnol.*, 2013, **171** (1), P. 63–71.
[33] Lv C., Di W., et al. Luminescent $CePO_4$:Tb colloids for H_2O_2 and glucose sensing. *Analyst*, 2014, **139** (18), P. 4547–4555.
[34] Tanaka S., Kaneti Y.V., et al. Mesoporous Iron Oxide Synthesized Using Poly(styrene-b-acrylic acid-b-ethylene glycol) Block Copolymer Micelles as Templates for Colorimetric and Electrochemical Detection of Glucose. *ACS Appl. Mater. Interfaces*, 2018, **10** (1), P. 1039–1049.
[35] Shiralizadeh Dezfuli A., Ganjali M.R., Norouzi P. Facile sonochemical synthesis and morphology control of CePO(4) nanostructures via an oriented attachment mechanism: application as luminescent probe for selective sensing of Pb^{2+} ion in aqueous solution. *Mater. Sci. Eng. C Mater. Biol. Appl.*, 2014, **42**, P. 774–781.
[36] Han K.N., Choi J.S., Kwon J. Gold nanozyme-based paper chip for colorimetric detection of mercury ions. *Sci. Rep.*, 2017, **7** (1), P. 1–7.
[37] Bhattacharjee R., Tanaka S., et al. Porous Nanozymes: Peroxidase-Mimetic Activity of Mesoporous Iron Oxide for Calorimetric and Electrochemical Detection of Global DNA Methylation. *J. Mater. Chem. B*, 2018, **6**, P. 4783–4791.
[38] Maji S.K., Mandal A.K., et al. Cancer Cell Detection and Therapeutics Using Peroxidase-Active Nanohybrid of Gold Nanoparticle-Loaded Mesoporous Silica-Coated Graphene. *ACS Appl. Mater. Interfaces*, 2015, **7**, P. 9807–9816.
[39] Ansari A.A., Solanki P.R., Malhotra B.D. Hydrogen peroxide sensor based on horseradish peroxidase immobilized nanostructured cerium oxide film. *J. Biotechnol.*, 2009, **142** (2), P. 179–184.
[40] Zhidkova T.V., Proskurnina E.V., et al. Determination of superoxide dismutase and SOD-mimetic activities by a chemical system: Co^{2+}/H_2O_2/lucigenin. *Anal. Bioanal. Chem.*, 2011, **401** (1), P. 381–386.
[41] Iketani M., Ohsawa I. Molecular Hydrogen as a Neuroprotective Agent. *Curr. Neuropharmacol.*, 2017, **15** (2), P. 324–331.
[42] Xue Y., Luan Q., et al. Direct Evidence for Hydroxyl Radical Scavenging Activity of Cerium Oxide Nanoparticles. *J. Phys. Chem.*, 2011, **115** (11), P. 4433–4438.
[43] Schlick S., Danilczuk M., et al. Scavenging of Hydroxyl Radicals by Ceria Nanoparticles: Effect of Particle Size and Concentration. *J. Phys. Chem. C*, 2016, **120** (12), P. 6885–6890.
[44] Popov A.L., Scherbakov A.B., et al. Cerium dioxide nanoparticles as third-generation enzymes (nanozymes). *Nanosystems: Phys. Chem. Math.*, 2017, **8** (6), P. 760–781.
[45] Linnane A.W., Kios M., Vitetta L. Healthy aging: regulation of the metabolome by cellular redox modulation and prooxidant signaling systems: the essential roles of superoxide anion and hydrogen peroxide. *Biogerontology*, 2007, **8** (5), P. 445–467.
[46] Spivak N.Y., Shepel E.A., et al. Ceria Nanoparticles Boost Activity of Aged Murine Oocytes. *Nano Biomedicine and Engineering*, 2012, **4**, P. 188–194.
[47] Courbiere B., Auffan M., et al. Ultrastructural interactions and genotoxicity assay of cerium dioxide nanoparticles on mouse oocytes. *Int. J. Mol. Sci.*, 2013, **14** (11), P. 21613–21628.
[48] Smith R.A., Murphy M.P. Mitochondria-targeted antioxidants as therapies. *Discov. Med.*, 2011, **11** (57), P. 106–114.
[49] Liu Y., Shi J. Antioxidative nanomaterials and biomedical applications. *Nano Today*, 2019, **27**, P. 146–177.
[50] Jiang D., Ni D., et al. Nanozyme: new horizons for responsive biomedical applications. *Chem. Soc. Rev.*, 2019, **48** (14), P. 3683–3704.